NeuroMolecular Medicine (2024) 26:36
https://doi.org/10.1007/s12017-024-08802-4

RESEARCH

Dysregulated Purinergic Signalling in Fragile X Syndrome Cortical Astrocytes

Kathryn E. Reynolds[2] · Matthew Napier[1,2] · Fan Fei[3,4] · Kirk Green[3] · Angela L. Scott[1,2]

Received: 15 July 2024 / Accepted: 20 August 2024

Abstract

The symptoms of fragile X syndrome (FXS), caused by a single gene mutation to *Fmr1*, have been increasingly linked to disordered astrocyte signalling within the cerebral cortex. We have recently demonstrated that the purinergic signalling pathway, which utilizes nucleoside triphosphates and their metabolites to facilitate bidirectional glial and glial-neuronal interactions, is upregulated in cortical astrocytes derived from the *Fmr1* knockout (KO) mouse model of FXS. Heightened *Fmr1* KO P2Y purinergic receptor levels were correlated with prolonged intracellular calcium release, elevated synaptogenic protein secretion, and hyperactivity of developing circuits. However, due to the relative lack of sensitive and reproducible quantification methods available for measuring purines and pyrimidines, determining the abundance of these factors in *Fmr1* KO astrocytes was limited. We therefore developed a hydrophilic interaction liquid chromatography protocol coupled with mass spectrometry to compare the abundance of intracellular and extracellular purinergic molecules between wildtype and *Fmr1* KO mouse astrocytes. Significant differences in the concentrations of UDP, ATP, AMP, and adenosine intracellular stores were found within *Fmr1* KO astrocytes relative to WT. The extracellular level of adenosine was also significantly elevated in *Fmr1* KO astrocyte-conditioned media in comparison to media collected from WT astrocytes. Glycosylation of the astrocyte membrane-bound CD39 ectonucleotidase, which facilitates ligand breakdown following synaptic release, was also elevated in *Fmr1* KO astrocyte cultures. Together, these differences demonstrated further dysregulation of the purinergic signalling system within *Fmr1* KO cortical astrocytes, potentially leading to significant alterations in FXS purinergic receptor activation and cellular pathology.

Keywords Purines · Pyrimidines · Astrocytes · Fragile X syndrome

Abbreviations

CNS	Central nervous system
FXS	Fragile X syndrome
ATP	Adenosine triphosphate
ADP	Adenosine diphosphate
AMP	Adenosine monophosphate
UTP	Uridine triphosphate
UDP	Uridine diphosphate
UMP	Uridine monophosphate
NMP	Nucleoside monophosphate
NDP	Nucleoside diphosphate
CD39	Ectonucleoside triphosphate diphosphohydrolase-1
CD73	Ecto-5′-nucleotidase

Introduction

During neuronal development, glial cells play critical roles in many aspects of the growth and establishment of neural networks. Astrocytes in particular are integral for regulating neuronal extension, synaptic formation, and circuitry homeostasis via reciprocal astrocyte-neuronal signalling systems within the central nervous system (CNS) (reviewed in Gradisnik & Velnar, 2023). Indeed, prior to the establishment of neural circuits, neurons must first be prompted by astrocytes to undergo a developmental switch that allows

✉ Angela L. Scott
angela.scott@uoguelph.ca

1 Department of Molecular and Cellular Biology, University of Guelph, 488 Gordon St., Guelph, ON, Canada

2 Department of Pathology and Molecular Medicine, McMaster University, Hamilton, ON, Canada

3 McMaster Regional Centre for Mass Spectrometry, McMaster University, Hamilton, ON, Canada

4 Moderna Inc., Norwood, MA, USA

Published online: 10 September 2024

them to form synapses (Barker & Ullian, 2008). In addition, astrocytes regulate the timing of structural synapse formation across brain regions, as well as the activity and function of synapses once formed (Liu et al. 1996; Pfrieger and Barres 1997; Li et al. 1999; Ullian et al. 2001). Given this, it is not surprising that astrocyte dysfunction has been associated with neurodevelopmental disorders characterized by either morphological or functional synaptic abnormalities, such as autism spectrum disorders (ASDs).

In many ASDs, genetic mutations lead to either the enhanced formation or reduced elimination of dendritic spines that cause greater densities of synaptic connections within the developing CNS (Tang et al., 2014; Guang et al., 2018). In fragile X syndrome (FXS), the leading monogenic cause of intellectual disability and ASD, higher densities of dendritic spines with immature morphologies and excitatory activity result in hyperexcitable cortical connections, sensory hyperresponsivity, attention deficit, and seizures (Farzin et al., 2006; Musumeci et al., 1999). In FXS, an expansion mutation in the *Fmr1* gene results in the absence of the fragile X messenger ribonucleoprotein (FMRP) in both neurons and astrocytes (Pieretti et al., 1991; Sutcliffe et al., 1992; Turner et al., 1996; Verkerk et al., 1991; Youings et al., 2000). Deletion of FMRP in astrocytes specifically affects the expression and release of synaptogenic factors, glutamate transmission, and neuronal morphology, as well as the activity and function of neuronal circuits (Cheng et al., 2016; Higashimori et al., 2016; Hodges et al., 2017; Jacobs & Doering, 2010; Wallingford et al., 2017). While the astrocyte-mediated molecular mechanisms involved in FXS dysfunction continue to be elucidated, several studies have demonstrated a potential role for the purinergic signalling system.

Gliotransmission of purines and pyrimidines (ex. ATP, UTP) and their metabolites facilitate widespread astrocyte-astrocyte and astrocyte-neuron communication within the CNS (Abbracchio et al., 2009). This communication is driven by the activation of two large receptor families, P1 and P2, that are expressed by both astrocytes and neurons, and classified according to their structure and ligand affinity. The P1 purinergic receptor family contains four members, A_1, A_{2A}, A_{2B}, and A_3, which are all metabotropic and bind adenosine. The P2 family is subdivided into ionotropic P2X receptors ($P2X_{1–7}$) and metabotropic P2Y receptors ($P2Y_{1,2,4,6,11–14}$) that are activated by nucleoside di- and triphosphates to increase intracellular calcium levels and promote signal transduction (Abbracchio et al., 2009). The uridine-based signalling ligands utilized by P2Y receptors are generated primarily by astrocytes through a combination of de novo synthesis pathways and the action of intracellular kinases that transfer phosphate residues from ATP to form UMP, UDP, and UTP (Dobolyi et al., 2011). Using an *Fmr1* knockout (KO) mouse model of FXS, our work has demonstrated that ATP/UTP-specific $P2Y_2$ and UDP/UTP-sensitive $P2Y_6$ receptor levels are elevated in *Fmr1* KO cortical astrocytes and correspond with prolonged *Fmr1* KO astrocyte activation, secretion of synaptogenic protein TSP-1, and hyperexcitability of neuronal circuits (Reynolds et al., 2021, 2024). Cortical astrocytes derived from FXS patients also exhibit elevated activation in response to ATP stimulus, further supporting a purinergic link to FXS astrocyte pathogenesis (Ren et al., 2023).

While our understanding of purinergic receptors in disorders such as FXS continues to expand, relatively little is known about the production, secretion, or metabolism of the purine or pyrimidine ligands. ATP/UTP nucleotides are known to stimulate the release of nucleoside triphosphates by astrocytes in an autocrine manner that can further drive activation of both glial and neuronal purinergic receptors (Abbracchio et al., 2009). Unbound ATP and UTP are rapidly hydrolysed to their di- and monophosphate forms by the astrocyte membrane-bound ectonucleoside triphosphate diphosphohydrolase enzyme CD39; while CD73, or ecto-5′-nucleotidase, removes single phosphates from AMP and UMP to produce adenosine and uridine (Fig. 1) (Dobolyi et al., 2011; Zimmermann, 1996). Purines and pyrimidines can also undergo re-uptake via astrocyte nucleoside

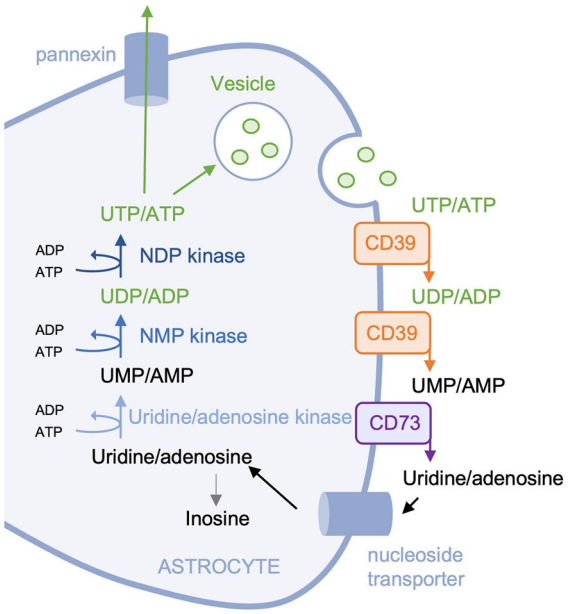

Fig. 1 Metabolism of adenosine- and uridine-based nucleosides and nucleotides. Astrocytes produce, secrete, and internalize purine and pyrimidine metabolites through the action of intracellular or membrane-bound enzymes, as well as pannexin channels and nucleoside transporters, respectively. ATP, adenosine triphosphate; UTP, uridine triphosphate; ADP, adenosine diphosphate; UDP, uridine diphosphate; AMP, adenosine monophosphate; UMP, uridine monophosphate; NMP, nucleoside monophosphate; NDP, nucleoside diphosphate; CD39, ectonucleoside triphosphate diphosphohydrolase-1; CD73, ecto-5'-nucleotidase

transporters for recycling and re-release (Lie et al., 1999; Wink et al., 2003). The action of astrocyte-based ectonucleotidases and transporters thereby helps to modulate ligand availability for both P2X and P2Y receptors, as well as those of the P1 receptor family. In this study, we explored the extent of purinergic dysregulation in FXS astrocytes by utilizing hydrophilic interaction liquid chromatography (HILIC) coupled with mass spectrometry (MS) to compare the intracellular and extracellular levels of purinergic metabolites by wildtype (WT) versus *Fmr1* KO mouse astrocytes. In addition, we also investigated the expression of astrocyte-bound CD39 and CD73 ectonucleotidases responsible for the extracellular metabolism of secreted ATP and UTP. Our findings demonstrate significant variations in purine production and metabolism in *Fmr1* KO astrocytes and support previous reports of purinergic signalling dysregulation in FXS.

Methods

Animals

Two genotypes of mice, wildtype (WT) and *Fmr1*$^{-/-}$ (Fmr1 KO; FVB.129P2[B6]-*Fmr1*^{tm1Cgr}), were bred and housed at the McMaster Health Sciences Central Animal Facility. All mouse housing, handling, and euthanization protocols followed the standards set by the Canadian Council on Animal Care and were authorized by the McMaster Animal Ethics Board (Animal Utilization Protocol 17-04-11). Pups of both sexes were euthanized by decapitation at postnatal day (P) 1–3 for astrocyte dissection and primary culture.

Primary Astrocyte Culture

WT and *Fmr1* KO primary cortical astrocyte cultures were prepared and maintained following protocols described previously by Jacobs and Doering (2009). Six cortical hemispheres, obtained from three postnatal day (P) 1-3 mouse pups, were pooled per genotype to form a single primary culture (n). Cells of the developing cerebral cortex were isolated by removing the hippocampus and meninges from each cortical hemisphere under a Zeiss Stemi SR stereo microscope (Carl Zeiss, Oberkochen, Germany), then dissociating cortical tissue in ice-cold Hanks' buffered saline solution (HBSS; Invitrogen, Waltham, MA, USA) with 1 mg/mL DNase (Roche Applied Science) and 0.25% trypsin (Invitrogen). Cells were plated in a glial-selective medium consisting of minimum essential medium (Gibco, Waltham, MA, USA) supplemented with 10% horse serum (Gibco) and 0.6% D-(+)-glucose (Sigma-Aldrich, St. Louis, MO, USA), and were maintained in a humidified incubator at 37 °C and 5% CO_2 (NuAire, Plymouth, MN, USA). Primary cultures received half media changes every 2–3 days, starting at 24h post-dissection, until cells were 75–90% confluent (~ 6–8 days).

After reaching 75–90% confluence, primary astrocyte cultures intended for liquid chromatography/mass spectrometry (LC/MS) were lifted with 0.05% trypsin-ethylenediaminetetraacetic acid (trypsin–EDTA; Gibco) for reseeding. Astrocytes were reseeded in six-well plates (Corning, NY, USA) pre-coated with 1 mg/mL poly-L-lysine (Sigma-Aldrich) and 10 µg/mL laminin (Invitrogen), at a density of 85 000 cells/well. After 24h, glial media were replaced with a serum-free glial media comprised of minimum essential media (Gibco) plus 0.6% D-(+)-glucose (Sigma-Aldrich), then cultures were maintained at 37 °C and 5% CO_2 for an additional 48 h.

Liquid Chromatography/Mass Spectrometry Sample Preparation for Intracellular Metabolites

For sample collection, plates were placed on ice and washed 2 × with ice-cold phosphate buffered saline (Gibco, Waltham, MA, USA) to halt ectonucleotidase activity. All six wells per plate were collected and pooled per sample to obtain sufficient quantities for nucleoside triphosphate detection, while a seventh well was collected to obtain a representative cell count for normalization. Astrocytes intended for LC/MS were mechanically lifted with a cell scraper (Corning) in 500 µL ice-cold LC/MS-grade methanol (Fisher Scientific, Waltham, MA, USA), while those intended for representative cell counts were lifted with 0.05% trypsin–EDTA. LC/MS cell suspensions were vortexed vigorously for 2 min, then stored at -80 °C until extraction.

Isotopically labelled adenosine-$^{13}C_5$ (Toronto Research Chemicals, North York, ON, Canada) was added to each cell suspension to act as an internal standard, achieving a final concentration of 2.5 ng/µL. Cell suspensions were vigorously vortexed for 2 min and centrifuged at 10,000 rpm for 5 min (4 °C), then supernatants were retained for LC/MS analysis. The extraction process was repeated twice with an additional 500 µL methanol, for a total of 3 pooled extractions per sample. The final pooled sample was dried with nitrogen gas and stored at − 80 °C until analysis. Samples were resuspended in 5 mM NH_4OAc (50 µL; Sigma-Aldrich) immediately prior to LC/MS.

Solid Phase Extraction (SPE) for Extracellular Metabolites

For detection of secreted nucleotides, each confluent primary astrocyte culture was passaged (as above) and replated into two T75 flasks. The cultures were maintained for approximately 4 additional days in vitro (DIV) or until they reached > 75% confluence. Glial media was then replaced with 6 mL of serum-free glial media with 100 µM NTPDase inhibitor ARL 67156 trisodium salt (Tocris) per flask and

incubated for 48 h. The media was then collected and pooled from both flasks per experimental sample. Adenosine-$^{13}C_5$ was added to each sample (2.755 µL of 100 µM stock) to act as an internal standard. To normalize samples to corresponding cell counts, astrocytes were removed from T75 flasks, centrifuged for 5 min (1500 rpm), and resulting pellets were resuspended in 1 mL of glial media. A small aliquot of the cell suspension was extracted, and cell numbers were analysed using a hemocytometer under 10X magnification.

A STRATA X-AW SPE column was connected to a vacuum manifold, which applied ~ 5 mmHg of vacuum pressure. The column was first conditioned with 1 mL each of MS-grade methanol (MeOH), 2:25:73 formic acid/MeOH/H_2O, and H_2O alone, and positioned over a collection tube. Astrocyte-conditioned media samples were added to the column at a rate of 1 drop/sec. The column was thoroughly washed with 1 mL MS-grade H_2O, the vacuum dried for 5 min prior to sample elution in 1 mL 2:98 NH_4OH/methanol. Collected samples were flash frozen in liquid nitrogen and stored at -80°C prior to lyophilization using a 6L Labconco FreeZone® Freeze Dryer System (Centre for Microbial Chemical Biology, McMaster University). Immediately prior to LC/MS, lyophilized samples were reconstituted in 30 µL of 5 mM NH_4OAc (MS-grade) and transferred to spring loaded inserts for appropriate MS autosampler loading.

Liquid Chromatography/Mass Spectrometry

A Luna NH_2 HILIC column with dimensions of 2.0 × 150 mm, 100 Å pore size, and 5 µm particle size (Cat# 00F-4378-B0, Phenomenex, Torrance, CA, USA) was utilized to separate purinergic targets for analysis. LC was performed on an Agilent 1260 HPLC system with a flow rate of 0.4 mL/min and an injection volume of 2 µL. Nucleoside mono-, di-, and triphosphates, with the exception of UMP, were able to be separated using the following aqueous and organic mobile phases: (A) 100 mM ammonium acetate (NH_4OAc; Sigma Aldrich) in water, adjusted to pH 9 with ammonium hydroxide (NH_4OH; Caledon); and (B) 100% acetonitrile (CH_3CN; Fisher Scientific), respectively. Adenosine, uridine, cytidine, and UMP were poorly detected using these parameters but were robustly detected when the concentration of mobile phase A was reduced to 10 mM NH_4OAc (pH 9). As this lower concentration of NH_4OAc could not be optimized to produce sharp nucleoside triphosphate peaks, samples were run twice, first with A: 100 mM NH_4OAc (pH 9) to detect ATP, ADP, AMP, UTP, UDP, and inosine, and again with A: 10 mM NH_4OAc (pH 9), to permit quantification of UMP, adenosine, uridine, and cytidine. The same LC/MS gradient was utilized for both applications and is summarized in Table 1. The LC system was paired with an Agilent 6550 iFunnel Q-TOF Mass Spectrometer (Agilent, Santa Clara, CA, USA) for purinergic detection.

Table 1 Optimized gradient utilized for LC/MS nucleotide analysis

Time (min)	Mobile phase	
	A (%)	B (%)
0	5	95
0.5	5	95
5.5	50	50
5.6	92	8
10	95	5
15	95	5
15.1	5	95
30	5	95

MS parameters included negative electrospray ionization, and high sensitivity detection with 2GHz extended dynamic range.

Prior to sample analysis, ESI- source parameters were optimized with authentic purinergic standards (Sigma-Aldrich). The following purinergic targets were detected at the specified observed m/z and retention times: ATP (505.9985 m/z; 8.7 min), ADP (426.0221 m/z; 8.4 min), AMP (346.0558 m/z; 7.9 min), UTP (482.9613 m/z; 8.5 min), UDP (402.9949 m/z; 5.7 min), UMP (323.0286 m/z; 7.7 min), adenosine (266.0895 m/z; 4.2 min), uridine (243.0623; 4.2 min), cytidine (242.0782; 5.7 min), inosine (267.0735 m/z; 5.1 min), and the internal standard adenosine-$^{13}C_5$ (271.1068 m/z). Within each genotype, the experimental sample consisted of 6–7 individual cultures ($n = 6$ or 7) prepared from 4 separate litters and run in triplicate. Selected targets were identified using Agilent MassHunter Qualitative Analysis B.07.00 software (Agilent), then analysed using Agilent MassHunter Quantitative Analysis B.07.01 software (Agilent). Mean nucleoside abundance was normalized to representative cell counts, as well as to the relative abundance of adenosine-$^{13}C_5$ internal standard.

Western Blotting

After reaching 75–90% confluence, primary astrocyte cultures intended for western blotting were lifted with 0.05% trypsin–EDTA and pelleted, then flash frozen in liquid nitrogen and stored at -80°C until homogenization. A total of 15 WT ($n = 15$) and 14 *Fmr1* KO ($n = 14$) samples were used for CD39 western blotting, and 8 samples per genotype ($n = 8$) were used for CD73 western blotting, obtained from individual cultures prepared from separate litters. Samples were homogenized on ice in brain extraction buffer (25 mM HEPES pH 7.3, 150 mM KCl, 8% glycerol, 0.1% NP-40, one Roche ULTRA protease inhibitor tablet, and one Roche PhoSTOP phosphatase inhibitor tablet) (Reynolds et al., 2021), and then total protein content was quantified within lysates (DC protein assay; BioRad, Mississauga, ON, Canada) to determine gel loading dilutions.

Western blotting samples were prepared with Laemmli sample buffer plus 2.5% ß-mercaptoethanol (BioRad) to achieve a dilution of 10 µg protein per lane. Samples were run on polyacrylamide TGX Stain-Free 4–12% gradient gels (BioRad) to separate proteins, activated with UV light for 45 s to permit visualization of "total protein" (tryptophan), then transferred to polyvinylidene difluoride (BioRad) membranes. Stain-free total protein loading control images were acquired using a ChemiDoc imaging system (BioRad), then membranes were blocked with 5% non-fat milk for 1 h. Primary antibodies against CD39 (rabbit monoclonal; 1:500; Abcam, Cambridge, UK Cat# ab223842, RRID:AB_2889212) or CD73 (mouse monoclonal; 1:500; R7D Systems, Minneapolis, MN, USA Cat# MAB57951) were applied overnight (4 °C), followed by the corresponding secondary antibodies donkey anti-rabbit horseradish peroxidase (1:2500; GE Healthcare, Chicago, IL, USA) or donkey anti-mouse horseradish peroxidase (1:5000; GE Healthcare). Bands for astrocyte membrane-bound CD39 were detected at ~ 75 and ~ 52 kDa, corresponding to glycosylated (active) and unglycosylated (immature) forms of the enzyme, respectively (Zhong et al., 2001). Membrane-bound glycosylated CD73 was detected at ~ 62 kDa (Adzic & Nedeljkovic, 2018; Zhou et al., 2019). Membranes were developed using Clarity MAX enhanced chemiluminescence (ECL) substrate (BioRad), and chemiluminescence images were acquired using the ChemiDoc imaging system (BioRad). Densitometry was performed using ImageLab 6.0.1 software (BioRad) to normalize bands of interest to the density of total protein bands.

Statistics

All statistical analyses were conducted using GraphPad Prism 8.0 software (GraphPad Software, San Diego, CA, USA). Comparisons between WT and *Fmr1* KO are expressed as fold change relative to WT means and were obtained using unpaired two-tailed t tests with significance at $p < 0.05$. For the metabolite analysis in WT and KO astrocyte-conditioned media, One-Way ANOVA was used with Tukey's posthoc multiple comparison test, comparing each mean. Relationships of interest were annotated, with $p < 0.05$ indicating significance.

Results

Intracellular UDP is Elevated in Fmr1 KO Astrocytes

Here, we utilized a hydrophilic interaction liquid chromatography protocol paired with mass spectrometry (HILIC-LC/MS) to detect intracellular purinergic signalling molecules within *Fmr1* KO and WT primary astrocytes. The internal standard adenosine-$^{13}C_5$ was used to normalize all ligand measurements and showed good reproducibility during the LC/MS sequence (data not shown). We observed several differences in intracellular nucleoside tri-, di-, and monophosphate abundance. Within the uridine-based family of ligands, intracellular UTP levels were unchanged in WT vs *Fmr1* KO astrocytes ($n = 6$, $p = 0.2673$; Fig. 2A, B), while levels of intracellular UDP were elevated in *Fmr1* KO astrocytes relative to WT ($n = 6$, $p = 0.0118$; Fig. 2C, D). The abundance of astrocyte intracellular UMP was also

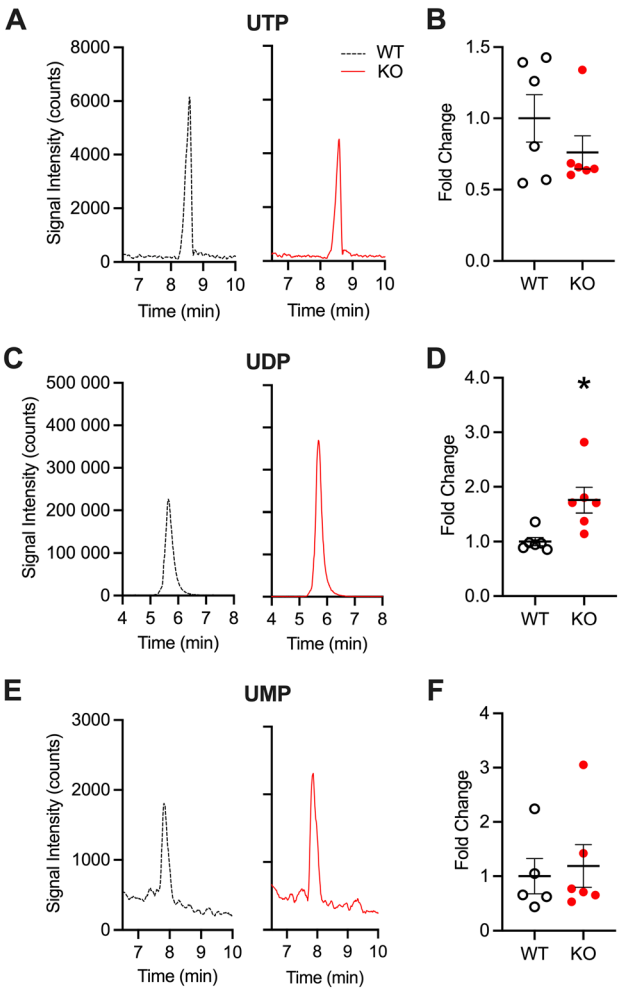

Fig. 2 LC/MS quantification of intracellular UTP, UDP, and UMP in WT and *Fmr1* KO primary cortical astrocytes. Representative extracted ion chromatograms of WT and *Fmr1* KO astrocyte intracellular UTP (**A**), UDP (**C**), and UMP (**E**). Relative abundance of intracellular UTP (**B**), UDP (**D**), and UMP (**F**) in WT and *Fmr1* KO cultured astrocytes, showing increased UDP levels in *Fmr1* KO astrocytes. Abundance is presented as fold change relative to mean WT signal intensity and is normalized to both representative cell count and adenosine-$^{13}C_5$ internal standard signal intensity. Data presented as means ± SEM. $n = 6$, with the exception of WT UMP $n = 5$; *$p < 0.05$

unchanged between genotypes (WT $n=5$/*Fmr1* KO $n=6$, $p=0.7292$; Fig. 2E, F).

Intracellular ATP and Adenosine are Reduced in Fmr1 KO Astrocytes

In contrast, the adenosine-based family of ligands showed additional differential patterns of intracellular levels between WT and *Fmr1* KO astrocytes. Intracellular ATP levels were notably reduced in *Fmr1* KO astrocytes in comparison to WT ($n=6$, $p=0.0425$; Fig. 3A, B), while intracellular ADP quantities did not change between genotypes ($n=6$, $p=0.4195$; Fig. 3C, D). However, intracellular levels of AMP were elevated in *Fmr1* KO astrocytes relative to WT ($n=6$, $p=0.0122$; Fig. 3E, F).

Intracellular nucleosides function as mono-, di-, and triphosphate precursors, while the nucleoside adenosine also acts as a gliotransmitter by binding to the P1 purinergic receptor subfamily to exert both excitatory and inhibitory effects. Here, adenosine abundance was reduced in *Fmr1* KO astrocytes (WT $n=5$/*Fmr1* KO $n=6$, $p=0.0494$; Fig. 4A, B). Intracellular levels of uridine ($n=5$, $p=0.6328$; Fig. 4C, D), inosine ($n=6$, $p=0.6111$; Fig. 4E, F), and cytidine (WT $n=5$/*Fmr1* KO $n=6$, $p=0.7062$; Fig. 4G, H) were unchanged.

Glycosylated CD39, but not CD73, is Elevated in Fmr1 KO Astrocytes

The abundance of purinergic ligands is governed in part by the action of the CD39 ectonucleoside triphosphate diphosphohydrolase enzyme, which breaks down UTP and ADP into their di- and monophosphate forms (Huang et al., 2021). Active CD39 is localized to the plasma membrane, where it was detectable at the commonly observed molecular weight of ~ 75 kDa. The ~ 52 kDa CD39 band we observed here has previously been shown to be indicative of an intracellularly localized form that only becomes active once it is glycosylated and incorporated within the plasma membrane (Zhong et al., 2001). Here, we found that the glycosylated, active form of CD39 (~ 75 kDa) was more highly expressed on the surface of *Fmr1* KO astrocytes ($n=14$) than WT ($p=0.0489$; $n=15$; Fig. 5A). In contrast, levels of the immature, unglycosylated form (~ 52 kDa) were reduced on the *Fmr1* KO astrocyte surface relative to WT ($p=0.0386$; Fig. 5A). Despite these differences, the total abundance of glycosylated plus immature CD39 did not differ between genotypes ($p=0.5799$), indicating that glycosylation rather than protein synthesis is altered in FXS. The membrane-bound ecto-5'-ectonucleotidase enzyme, also known as CD73, converts UMP into uridine and is therefore also important in regulating purinergic ligand availability. Here, no differences were observed in the level of

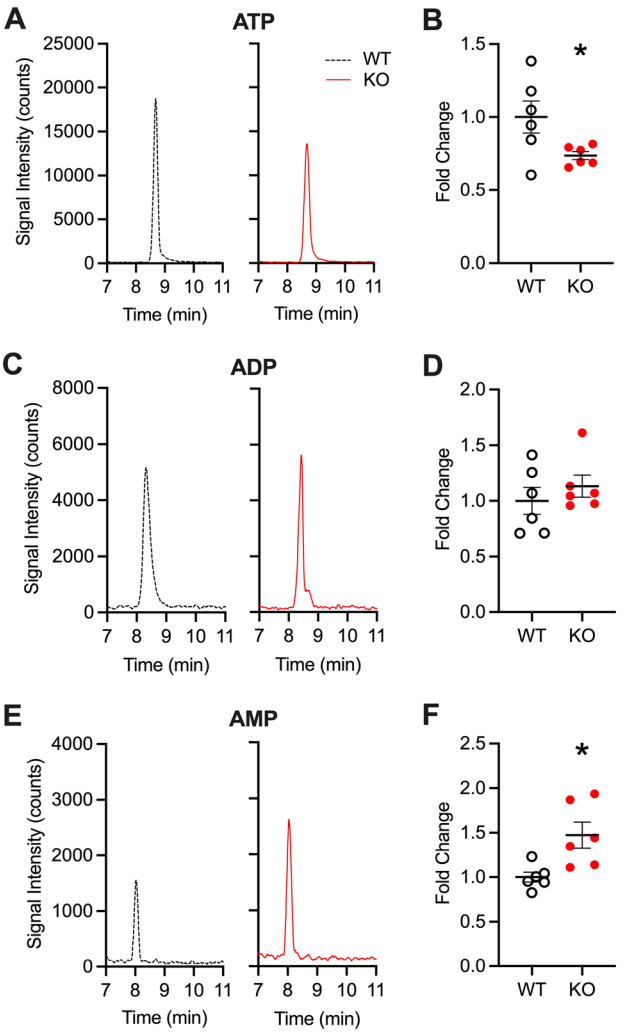

Fig. 3 LC/MS quantification of intracellular ATP, ADP, and AMP in WT and *Fmr1* KO primary cortical astrocytes. Representative extracted ion chromatograms of WT and *Fmr1* KO astrocyte intracellular ATP (**A**), ADP (**C**), and AMP (**E**). Relative abundance of intracellular ATP (**B**), ADP (**D**), and AMP (**F**) in WT and *Fmr1* KO cultured astrocytes, showing reduced ATP levels and elevated AMP levels in *Fmr1* KO astrocytes. Abundance is presented as fold change relative to mean WT signal intensity and is normalized to both representative cell count and adenosine-$^{13}C_5$ internal standard intensity. Data presented as means ± SEM. $n=6$; $^*p<0.05$

astrocyte-associated CD73 ($p=0.5185$; $n=8$) between WT and *Fmr1* KO cultures (Fig. 5B).

Secreted Adenosine Levels are Elevated by Fmr1 KO Cortical Astrocytes

Levels of extracellular purines and pyrimidines were also measured in the conditioned media of *Fmr1* KO and WT astrocyte cultures. Extracellular nucleosides are the result of either direct secretion by astrocytes or the metabolism of their phosphate bound precursors. Here, we found that

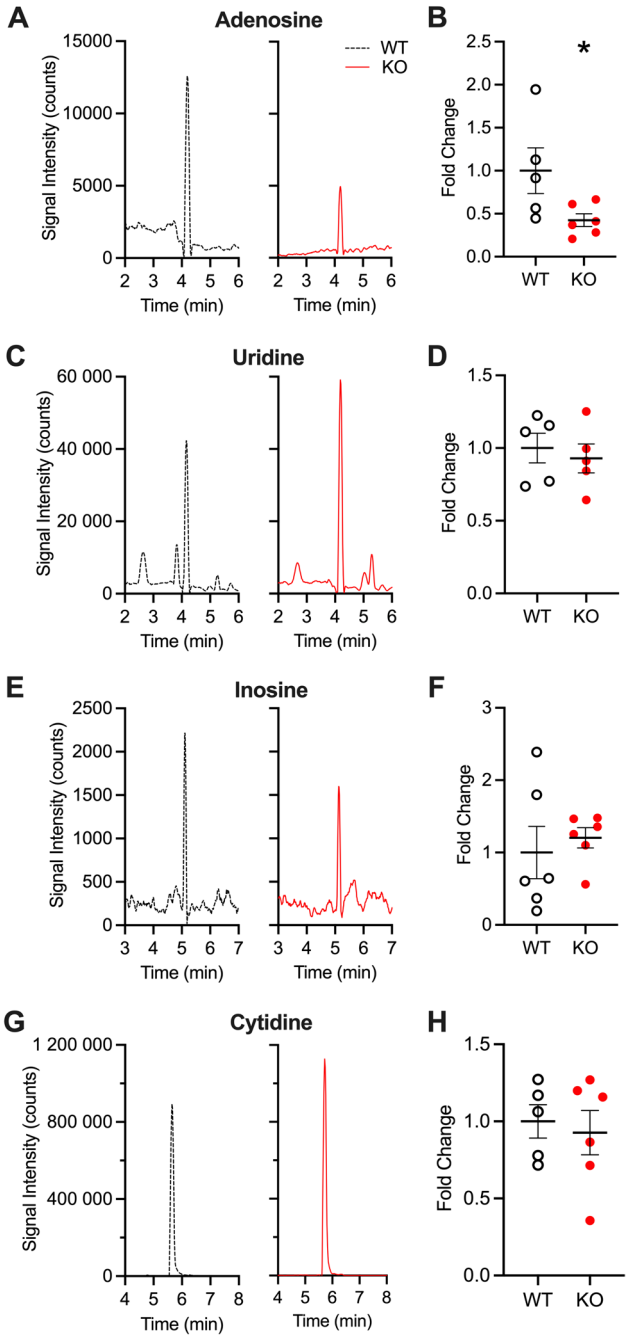

Fig. 4 LC/MS quantification of intracellular nucleosides in WT and *Fmr1* KO primary cortical astrocytes. Representative extracted ion chromatograms of adenosine (**A**), uridine (**C**), inosine (**E**), and cytidine (**G**). Relative abundance of intracellular adenosine (**B**), uridine (**D**), inosine (**F**), and cytidine (**H**) in WT and *Fmr1* KO cultured astrocytes, show decreased adenosine levels in *Fmr1* KO astrocytes only. Abundance is presented as fold change relative to mean WT signal intensity and is normalized to both representative cell counts and adenosine-$^{13}C_5$ internal standard signal intensity. Data presented as means ± SEM. WT $n=5$, with the exception of WT inosine $n=6$; *Fmr1* KO $n=6$; *$p<0.05$

the concentration of uridine present within WT astrocyte-conditioned media was significantly higher than the levels of other nucleosides, including adenosine ($p=0.0021$), inosine ($p=0.0029$), guanosine ($p=0.006$), and cytosine ($p=0.006$) (one-way ANOVA; Fig. 6A). Conversely, there were higher average concentrations of uridine present in media collected from *Fmr1* KO astrocytes in comparison to inosine ($p=0.0118$), guanosine ($p=0.0060$), and cytosine ($p=0.0061$), but not adenosine ($p=0.4721$) (one-way ANOVA; Fig. 6B). Across genotypic comparisons, only adenosine was measured in significantly higher concentrations in *Fmr1* KO astrocyte media ($n=5$) than in WT ($n=7$; $p=0.0462$; Fig. 6C). All other genotypic comparisons showed similar concentrations of uridine (WT $n=7$/KO $n=6$, $p=0.7578$; Fig. 6D), inosine (WT $n=6$/KO $n=6$, $p=0.8734$; Fig. 6D), guanosine (WT $n=7$/KO $n=6$, $p=0.5185$; Fig. 6D), and cytidine (WT $n=7$/KO $n=6$, $p=0.6918$; Fig. 6D) within the collected media of WT and *Fmr1* KO astrocyte cultures (via Student t tests).

Discussion

Recent research has shown that purinergic signalling pathways are elevated in *Fmr1* KO cortical astrocytes, which has functional consequences for astrocytic and neuronal excitation (Reynolds et al., 2021, 2024). To further elucidate the extent of purinergic astrocyte dysfunction, it is important to consider the secretion and metabolism of purinergic ligands by these cells. Here, we compared the levels of *Fmr1* KO and WT intracellular nucleoside triphosphates and successive metabolites using HILIC-LC/MS, either secreted or metabolized, within the media of WT and *Fmr1* KO astrocyte primary cultures. We confirmed that in addition to receptor expression differences reported previously, several nucleoside-based ligands for these receptors were also dysregulated in *Fmr1* KO astrocytes. This included significant differences in levels of UDP, ATP, AMP, and adenosine intracellular stores within *Fmr1* KO astrocytes, and increased concentrations of extracellular adenosine. In addition, *Fmr1* KO astrocytes showed enhanced levels of glycosylation of the membrane-bound CD39 ectonucleotidase, which is responsible for the metabolism of both ATP and UTP. Taken together, the loss of FMRP in astrocytes leads to widespread purinergic dysregulation affecting not only receptor expression but also the production and availability of several purines and pyrimidines.

Increased Intracellular UDP is Consistent with Elevated P2Y Activity in Fmr1 KO Astrocytes

One of the most prominent genotypic differences we observed in this study was a nearly twofold increase in *Fmr1*

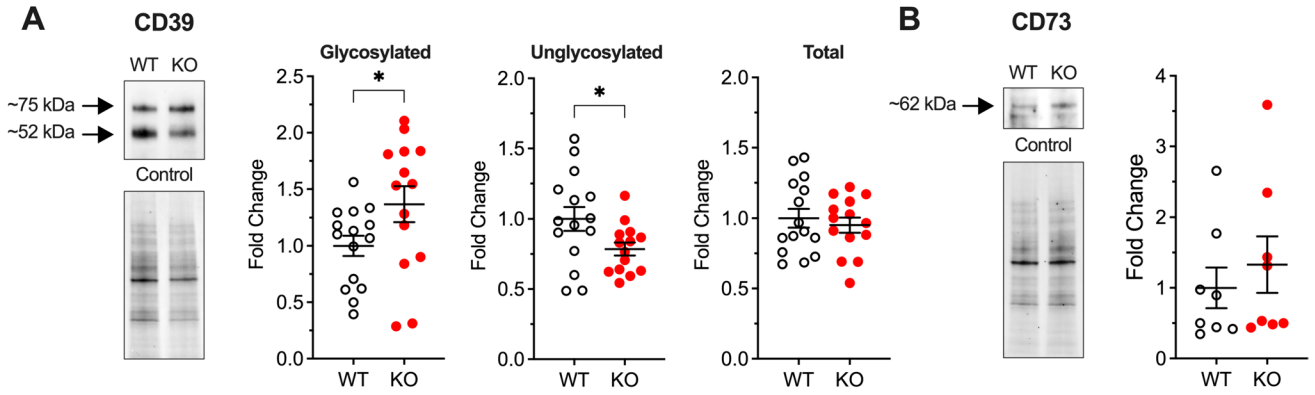

Fig. 5 Western blotting quantification of WT and *Fmr1* KO primary cortical astrocyte membrane-bound ectonucleotidases. **A.** Representative western blot of astrocyte membrane-bound CD39 ectonucleotidase and corresponding total protein control, showing bands for both glycosylated (~75 kDa) and unglycosylated (~52 kDa) CD39. **B.** Glycosylated (i.e. active) CD39 levels were elevated in *Fmr1* KO astrocyte cultures ($n=14$) relative to WT ($n=15$), while unglycosylated (*i.e.* immature) CD39 levels (**C**) were reduced in *Fmr1* KO; when both forms were added together, the total levels of CD39 were unchanged between genotypes. **D.** Representative western blot and corresponding total protein image of WT and *Fmr1* KO astrocyte-associated CD73. **E.** Astrocyte-bound CD73 was present at similar levels in WT and *Fmr1* KO ($n=8$) cultures. Enzyme abundance was normalized to total protein and presented as fold change relative to mean WT levels. Data presented as means ± SEM; $^{*}p<0.05$

KO astrocyte intracellular UDP relative to WT. This increase in UDP is particularly interesting given recent reports of pyrimidine dysregulation in FXS and ASD. Elevated levels of uridine, a UDP nucleoside precursor, were detected within the plasma of children with ASD (Adams et al., 2011). Circulating uridine has been previously correlated with cerebral UDP levels, as intravenously administered uridine has been shown to pass through the blood–brain barrier to increase the concentration of UDP within the mouse brain (Steculorum et al., 2015). Thus, the elevated plasma uridine in ASD is consistent with our findings of elevated UDP in *Fmr1* KO astrocytes. Increases to uridine or UMP via supplementation, dietary or otherwise, also result in elevated levels of UTP and CTP, which in turn raises phosphatide synthesis, synaptic membrane formation, and synaptic protein density (Wurtman et al., 2009). While we did not detect elevated UTP abundance in *Fmr1* KO compared to WT astrocytes, the fact that UTP is metabolized and secreted very quickly within these cells makes any changes difficult to detect. Given the enhanced growth of dendritic spines and the hyperactive circuitry reported in the *Fmr1* KO cortex, it is possible that enhancement of pyrimidine derivatives, such as UDP or UTP, in *Fmr1* KO astrocytes contributes to aberrant synaptogenesis.

The increased presence of astrocyte intracellular UDP also suggests the potential for substantial *Fmr1* KO UDP release to stimulate the activity of astrocytic or neuronal $P2Y_6$ receptors. UDP uniquely acts as a strong agonist of metabotropic $P2Y_6$ receptors, with weaker or negligible binding to other purinergic receptor types (Abbracchio et al., 2009). $P2Y_6$ receptors are in fact one of the two P2Y receptor types found to be elevated in *Fmr1* KO cortical astrocytes (Reynolds et al., 2021), so the increase in intracellular UDP may be indicative of upregulated $P2Y_6$-mediated signalling. Activation of $P2Y_6$ and other P2Y receptors leads to PLC/IP3-driven endoplasmic reticulum intracellular calcium release, thereby promoting the propagation of intercellular calcium waves, calcium-dependent gliotransmitter release, and transcription factor activation via signal transduction cascades including the MAPK, Akt, and STAT3 pathways (reviewed in Burnstock, 2009; Napier et al., 2023). Thus, the combination of increased receptor expression paired with increased intracellular ligand stores suggests the potential for widespread calcium wave propagation, neuronal firing, and modulation of gene expression, all of which are generally consistent with the FXS phenotype of cortical hyperexcitation.

Significant Alterations of Fmr1 KO Adenosine-Based Purinergic Signalling Molecules

The adenosine-based family of purinergic molecules was altered in *Fmr1* KO astrocytes, with significant dysregulations of the intracellular levels of ATP, AMP, and adenosine. Recent work has shown reduced ATP synthesis within the *Fmr1* KO cortex (D'Antoni et al., 2020), which is consistent with the reduced ATP levels we observed here. Mitochondria are important sources of ATP production, and our detection methods did not discriminate between intracellular ATP used for cellular metabolism versus gliotransmission. Mitochondrial dysfunction, including decreased mitochondrial fusion and elevated mitochondrial fragmentation in *Fmr1* KO neurons (Shen et al., 2019, 2023), as well as increased production of reactive oxygen species (ROS) in

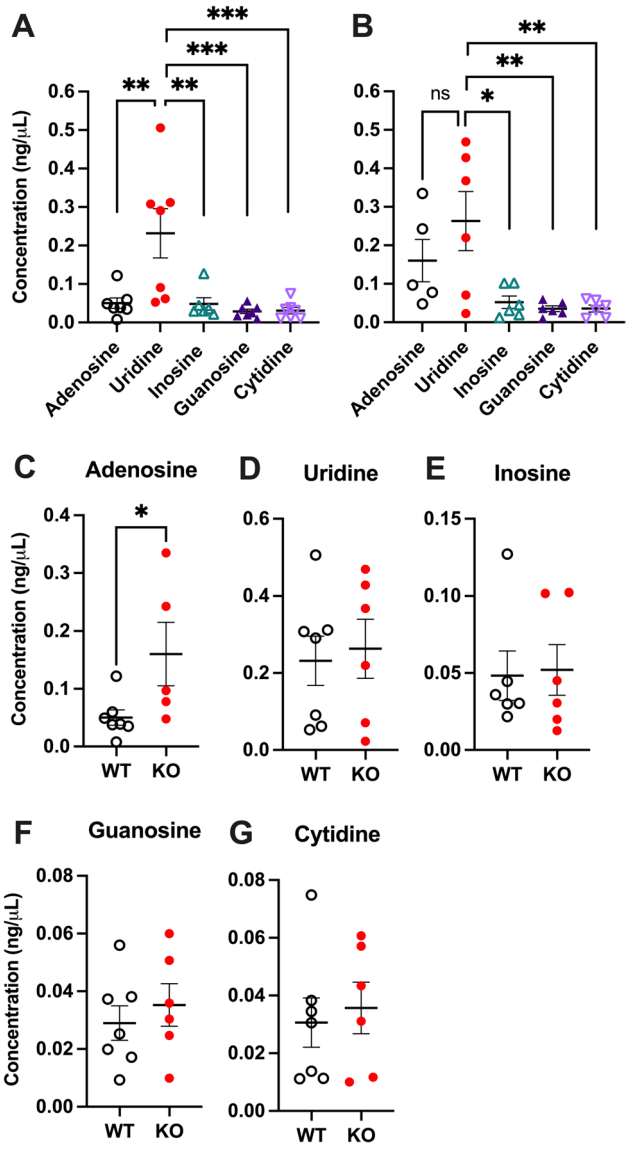

Fig. 6 LC/MS quantification of extracellular nucleosides in conditioned media of WT and *Fmr1* KO primary cortical astrocyte cultures. Relative abundance of each secreted factor within each culture genotype is given for WT (**A**) and *Fmr1* KO (**B**) astrocytes. Direct comparisons between secreted levels of adenosine (**C**), uridine (**D**), inosine (**E**), guanosine (**F**), and cytidine (**G**) from WT and *Fmr1* KO cultured astrocytes. Concentrations are normalized to both representative cell counts and adenosine-$^{13}C_5$ internal standard signal intensity. Data presented as means ± SEM. WT $n = 7$, with the exception of WT inosine $n = 6$; *Fmr1* KO $n = 6$, with the exception of KO adenosine $n = 5$; *$p < 0.05$; **$p < 0.01$; ***$p < 0.001$

Fmr1 KO astrocytes (Vandenberg et al., 2021, 2022), has been recently reported in the *Fmr1* KO model. Oxidative stress, arising from high calcium loading and the dysregulation of mitochondrial permeability, manifests elevations of cytoplasmic ROS and a depletion of ATP (reviewed in Brookes et al., 2004). Given the accumulating evidence for oxidative stress and mitochondrial dysfunction in FXS and related disorders, such as fragile X-associated tremor/ataxia syndrome, ATP reductions may not be surprising. Given the innumerable roles ATP plays within the cell, it is likely that both mitochondrial dependent and independent mechanisms contribute to the reduction of ATP in *Fmr1* KO astrocytes.

In terms of purine and pyrimidine biosynthesis and metabolism within *Fmr1* KO astrocytes, reduced intracellular ATP levels may also be the direct result of enhanced UDP formation, as both uridine kinase and UMP kinase utilize ATP as a substrate to promote UMP and UDP production, respectively. The same is true for elevations in AMP, as adenosine kinase also utilizes ATP to phosphorylate adenosine to AMP (as shown in Fig. 1). Another consideration is nucleoside or nucleotide transport and secretion. While the secretion of ATP from astrocytes could not be assessed directly due to rapid rates of metabolism, elevated levels of adenosine in the conditioned media of *Fmr1* KO astrocytes suggest that either adenosine-based nucleotides or nucleosides are released at greater capacities. ATP can be released from astrocytes via vesicular release, or connexin hemichannel and pannexin channel activation. Under pathological conditions, connexin-43, connexin-30, and pannexin-1 are permeable to ATP and lead to the secretion of nucleotides to either bind purinergic receptors or be efficiently metabolized by membrane-bound enzymes (Giaume et al., 2020). Extracellular adenosine is then cleared and replenished within the cell by equilibrative nucleoside transporters, such as ENT1 and ENT2, that mediate uptake by facilitated diffusion. In addition, nucleosides are recycled into astrocytes via CN2 sodium-dependent concentrative transporters that have a particularly strong affinity for adenosine (Peng et al., 2005). The increased concentration of extracellular adenosine within the *Fmr1* KO astrocyte media, in combination with reductions of both intracellular ATP and adenosine levels, suggests that the rate of ATP metabolism outpaces re-uptake of adenosine by *Fmr1* KO astrocytes.

Increased Glycosylation of CD39 Ectonucleotidase in Fmr1 KO Astrocytes

Membrane-bound ectonucleotidases control the strength and duration of purinergic agonism by metabolizing secreted gliotransmitters to facilitate their re-uptake by nucleoside transporters. Increased glycosylation of astrocyte membrane-bound CD39 further supports that ectonucleotidase-mediated nucleotide metabolism prior to re-uptake is enhanced in the FXS cortex. In the context of extracellular ATP metabolism, CD39 has been shown to more rapidly metabolize ATP than ADP. Extracellular ATP is almost completely metabolized within 30 min in vitro to produce a 40% accumulation of ADP; however, ADP is not converted to AMP until 80% of the initially released ATP had been metabolized, taking an additional 2.5 h (Wink et al., 2003).

Though the dynamics of UTP metabolism were not examined by Wink et al. (2003), ATP and UTP are both metabolized by the ectonucleotidase CD39, suggesting that UTP/UDP metabolism may follow a similar pattern. As receptors such as $P2Y_1$ and $P2Y_6$ have higher affinity for diphosphates than triphosphates (ADP > ATP and UDP > UTP, respectively) (von Kügelgen, 2019), the action of CD39 may therefore increase the likelihood that these receptors are agonised following nucleotide release. While our recent work suggests that aberrant activation of $P2Y_2$ receptors contributes to cellular pathology, such as hyperactivity of astrocytes and neurons, in the *Fmr1* KO mouse (Reynolds et al., 2024), further consideration of other receptor dysregulation (ex. $P2Y_6$) will help elucidate the impact of this signalling system in FXS.

Hydrophilic Interaction LC/MS is a Robust Method for Nucleoside Triphosphate Detection

Previous studies have successfully reported relative ATP concentrations using techniques such as ELISA or luciferase assays, but commercially available methodology for the reliable detection of UTP is much more limited. LC/MS approaches for UTP detection have also remained challenging due to significant restrictions in the optimization of the separation of hydrophilic analytes. Here, we used a NH2 column in HILIC mode that permitted polar and hydrophilic molecules to be temporarily retained on a polar stationary phase with a higher percentage of organic solvent and eluted with an aqueous mobile phase gradient (Alpert, 1990; Hemström & Irgum, 2006). HILIC has previously been utilized to detect UTP, ATP, and their metabolites with some success (Narayan, 2017), though detection of UTP was still limited (Galeano Garcia et al., 2019; Kong et al., 2018; Zhang et al., 2014). In contrast, our use of a basic and highly concentrated aqueous mobile phase (100 mM NH_4OAc pH 9) ensured the timely elution of ATP and UTP, while nucleosides were readily and reproducibly detected under lower aqueous phase concentrations (10 mM NH_4OAc pH 9). In addition, we optimized solid phase extraction from culture media prior to liquid chromatography in order to concentrate extracellular purine and pyrimidine metabolites while removing matrix interferences. In all, this work offers a novel methodology for the examination of astrocyte-mediated purinergic dysregulation and further elucidates the pathological changes to this signalling system in FXS.

Acknowledgements This work was supported by a grant to A. Scott from the Scottish Rite Charitable Foundation of Canada (#21107) that supports mental health research. K. Reynolds was funded by a Canadian Institutes of Health Research Canada Graduate Scholarship (CIHR CGS-D).

Authors Contributions K. Reynolds and A. Scott wrote the main manuscript. K. Reynolds and A. Scott prepared Figs. 1-5. M. Napier and A. Scott prepared Fig. 6. K. Reynolds, F. Fei, M. Napier, K. Green, and A. Scott were involved in data collection and experimental design contributing to Figs. 2, 3, 4, 5, and 6. All authors reviewed the manuscript. A. Scott received the grant for funding the project.

Availability of Data and Materials The data that support the findings of this study are available from the corresponding author upon reasonable request. No datasets were generated or analysed during the current study.

Declarations

Conflict of Interest The authors declare no competing interests.

Ethical Approval All animal experimental protocols were authorized by the McMaster Animal Ethics Board (Animal Utilization Protocol #21-02-06) and the University of Guelph Animal Ethics Board (Animal Utilization Protocol #5017) following Canadian Council on Animal Care policies.

Disclaimer Portions of this manuscript appear in the PhD thesis of K. Reynolds.

References

Abbracchio, M. P., Burnstock, G., Verkhratsky, A., & Zimmermann, H. (2009). Purinergic signalling in the nervous system: An overview. *Trends in Neurosciences, 32*(1), 19–29. https://doi.org/10.1016/j.tins.2008.10.001

Adams, J. B., Audhya, T., McDonough-Means, S., Rubin, R. A., Quig, D., Geis, E., Gehn, E., Loresto, M., Mitchell, J., Atwood, S., Barnhouse, S., & Lee, W. (2011). Nutritional and metabolic status of children with autism vs. neurotypical children, and the association with autism severity. *Nutrition & Metabolism (London), 8*(1), 34. https://doi.org/10.1186/1743-7075-8-34

Adzic, M., & Nedeljkovic, N. (2018). Unveiling the role of ecto-5′-nucleotidase/CD73 in astrocyte migration by using pharmacological tools. *Frontiers in Pharmacology, 9*, 153. https://doi.org/10.3389/fphar.2018.00153

Alpert, A. J. (1990). Hydrophilic-interaction chromatography for the separation of peptides, nucleic acids and other polar compounds. *Journal of Chromatography A, 499*, 177–196. https://doi.org/10.1016/S0021-9673(00)96972-3

Barker, A. J., & Ullian, E. M. (2008). New roles for astrocytes in developing synaptic circuits. *Communicative & Integrative Biology, 1*(2), 207–211. https://doi.org/10.4161/cib.1.2.7284.PMID:19513261;PMCID:PMC2686024

Cheng, C., Lau, S. K. M., & Doering, L. C. (2016). Astrocyte-secreted thrombospondin-1 modulates synapse and spine defects in the fragile X mouse model. *Molecular Brain, 9*, 74. https://doi.org/10.1186/s13041-016-0256-9

D'Antoni, S., de Bari, L., Valenti, D., Borro, M., Bonaccorso, C. M., Simmaco, M., Vacca, R. A., & Catania, M. V. (2020). Aberrant mitochondrial bioenergetics in the cerebral cortex of the Fmr1 knockout mouse model of fragile X syndrome. *Biological Chemistry, 401*(4), 497–503. https://doi.org/10.1515/hsz-2019-0221

Dobolyi, A., Juhasz, G., Kovacs, Z., & Kardos, J. (2011). Uridine function in the central nervous system. *Current Topics in Medicinal Chemistry, 11*(8), 1058–1067. https://doi.org/10.2174/156802611795347618

Farzin, F., Perry, H., Hessl, D., Loesch, D., Cohen, J., Bacalman, S., Gane, L., Tassone, F., Hagerman, P., & Hagerman, R. (2006). Autism spectrum disorders and attention-deficit/hyperactivity disorder in boys with the fragile X premutation. *Journal of*

Developmental and Behavioral Pediatrics, 27(2 Suppl), S137-144. https://doi.org/10.1097/00004703-200604002-00012

Galeano Garcia, P., Zimmermann, B. H., & Carazzone, C. (2019). hydrophilic interaction liquid chromatography coupled to mass spectrometry and multivariate analysis of the de novo pyrimidine pathway metabolites. *Biomolecules*. https://doi.org/10.3390/biom9080328

Gradisnik, L., & Velnar, T. (2023). Astrocytes in the central nervous system and their functions in health and disease: A review. *World Journal of Clinical Cases, 11*(15), 3385–3394. https://doi.org/10.12998/wjcc.v11.i15.3385. PMID: 37383914; PMCID: PMC10294192.

Guang, S., Pang, N., Deng, X., Yang, L., He, F., Wu, L., Chen, C., Yin, F., & Peng, J. (2018). Synaptopathology involved in autism spectrum disorder. *Frontiers in Cellular Neuroscience, 21*(12), 470. https://doi.org/10.3389/fncel.2018.00470.PMID:30627085;PMCID:PMC6309163

Hemström, P., & Irgum, K. (2006). Hydrophilic interaction chromatography. *Journal of Separation Science, 29*(12), 1784–1821. https://doi.org/10.1002/jssc.200600199

Higashimori, H., Schin, C. S., Chiang, M. S., Morel, L., Shoneye, T. A., Nelson, D. L., & Yang, Y. (2016). Selective deletion of astroglial FMRP dysregulates glutamate transporter GLT1 and contributes to fragile X syndrome phenotypes in vivo. *Journal of Neuroscience, 36*(27), 7079–7094. https://doi.org/10.1523/jneurosci.1069-16.2016

Hodges, J. L., Yu, X., Gilmore, A., Bennett, H., Tjia, M., Perna, J. F., Chen, C. C., Li, X., Lu, J., & Zuo, Y. (2017). Astrocytic contributions to synaptic and learning abnormalities in a mouse model of fragile X syndrome. *Biological Psychiatry, 82*(2), 139–149. https://doi.org/10.1016/j.biopsych.2016.08.036

Huang, Z., Xie, N., Illes, P., Di Virgilio, F., Ulrich, H., Semyanov, A., Verkhratsky, A., Sperlagh, B., Yu, S. G., Huang, C., & Tang, Y. (2021). From purines to purinergic signalling: molecular functions and human diseases. *Signal Transduction and Targeted Therapy, 6*, 162. https://doi.org/10.1038/s41392-021-00553-z

Jacobs, S., & Doering, L. C. (2009). Primary dissociated astrocyte and neuron co-culture. In L. C. Doering (Ed.), *Protocols for neural cell culture* (4th ed., pp. 269–284). Humana.

Jacobs, S., & Doering, L. C. (2010). Astrocytes prevent abnormal neuronal development in the fragile X mouse. *The Journal of Neuroscience, 30*(12), 4508–4514. https://doi.org/10.1523/jneurosci.5027-09.2010

Kong, Z., Jia, S., Chabes, A. L., Appelblad, P., Lundmark, R., Moritz, T., & Chabes, A. (2018). Simultaneous determination of ribonucleoside and deoxyribonucleoside triphosphates in biological samples by hydrophilic interaction liquid chromatography coupled with tandem mass spectrometry. *Nucleic Acids Research, 46*(11), e66–e66. https://doi.org/10.1093/nar/gky203

Li, Y. X., Schaffner, A. E., & Barker, J. L. (1999). Astrocytes regulate the developmental appearance of GABAergic and glutamatergic postsynaptic currents in cultured embryonic rat spinal neurons.*European Journal of Neuroscience, 11*(7), 2537–51.

Lie, A. A., Blümcke, I., Beck, H., Wiestler, O. D., Elger, C. E., & Schoen, S. W. (1999). 5'-Nucleotidase activity indicates sites of synaptic plasticity and reactive synaptogenesis in the human brain. *Journal of Neuropathology and Experimental Neurology, 58*(5), 451–458. https://doi.org/10.1097/00005072-199905000-00004

Liu, Q. Y., Schaffner, A. E., Li, Y. X., Dunlap, V., & Barker, J. L. (1996). Upregulation of GABAA current by astrocytes in cultured embryonic rat hippocampal neurons. *Journal of Neuroscience, 16*(9), 2912–23.

Musumeci, S. A., Hagerman, R. J., Ferri, R., Bosco, P., Bernardina, B. D., Tassinari, C. A., De Sarro, G. B., & Elia, M. (1999). Epilepsy and EEG findings in males with fragile X syndrome. *Epilepsia, 40*(8), 1092–1099. https://doi.org/10.1111/j.1528-1157.1999.tb00824.x

Napier, M., Reynolds, K., & Scott, A. L. (2023). Glial-mediated dysregulation of neurodevelopment in fragile X syndrome. *International Review of Neurobiology, 173*, 187–215. https://doi.org/10.1016/bs.irn.2023.08.005. Epub 2023 Sep 16 PMID: 37993178.

Narayan, V. (2017). *HPLC analysis of nucleotides* (Master of Applied Science (Research)). Queensland University of Technology

Pfrieger, F. W., & Barres, B. A. (1997). Synaptic efficacy enhanced by glial cells in vitro. *Science,* 277(5332), 1684–7.

Pieretti, M., Zhang, F. P., Fu, Y. H., Warren, S. T., Oostra, B. A., Caskey, C. T., & Nelson, D. L. (1991). Absence of expression of the FMR-1 gene in fragile X syndrome. *Cell, 66*(4), 817–822. https://doi.org/10.1016/0092-8674(91)90125-i

Ren, B., Burkovetskaya, M., Jung, Y., Bergdolt, L., Totusek, S., Martinez-Cerdeno, V., Stauch, K., Korade, Z., & Dunaevsky, A. (2023). Dysregulated cholesterol metabolism, aberrant excitability and altered cell cycle of astrocytes in fragile X syndrome. *Glia, 71*(5), 1176–1196. https://doi.org/10.1002/glia.24331. Epub 2023 Jan 3. PMID: 36594399; PMCID: PMC10023374.

Reynolds, K. E., Huang, E., Sabbineni, M., et al. (2024). Purinergic signalling mediates aberrant excitability of developing neuronal circuits in the Fmr1 knockout mouse model. *Molecular Neurobiology.* https://doi.org/10.1007/s12035-024-04181-w. PMID: 38652351.

Reynolds, K. E., Wong, C. R., & Scott, A. L. (2021). Astrocyte-mediated purinergic signaling is upregulated in a mouse model of fragile X syndrome. *Glia, 69*(7), 1816–1832. https://doi.org/10.1002/glia.23997

Shen, M., Sirois, C. L., Guo, Y., Li, M., Dong, Q., Méndez-Albelo, N. M., Gao, Y., Khullar, S., Kissel, L., Sandoval, S. O., Wolkoff, N. E., Huang, S. X., Xu, Z., Bryan, J. E., Contractor, A. M., Korabelnikov, T., Glass, I. A., Doherty, D., Birth Defects Research Laboratory, … Zhao, X. (2023). Species-specific FMRP regulation of RACK1 is critical for prenatal cortical development. *Neuron, 111*(24), 3988–4005. https://doi.org/10.1016/j.neuron.2023.09.014. Epub 2023 Oct 10. PMID: 37820724; PMCID: PMC10841112.

Shen, M., Wang, F., Li, M., Sah, N., Stockton, M. E., Tidei, J. J., Gao, Y., Korabelnikov, T., Kannan, S., Vevea, J. D., Chapman, E. R., & Zhao, X. (2019). Reduced mitochondrial fusion and Huntingtin levels contribute to impaired dendritic maturation and behavioral deficits in Fmr1-mutant mice. *Nature Neuroscience, 22*(3), 386–400. https://doi.org/10.1038/s41593-019-0338-y

Steculorum, S. M., Paeger, L., Bremser, S., Evers, N., Hinze, Y., Idzko, M., Kloppenburg, P., & Brüning, J. C. (2015). Hypothalamic UDP increases in obesity and promotes feeding via P2Y6-dependent activation of AgRP neurons. *Cell, 162*(6), 1404–1417. https://doi.org/10.1016/j.cell.2015.08.032

Sutcliffe, J. S., Nelson, D. L., Zhang, F., Pieretti, M., Caskey, C. T., Saxe, D., & Warren, S. T. (1992). DNA methylation represses FMR-1 transcription in fragile X syndrome. *Human Molecular Genetics, 1*(6), 397–400. https://doi.org/10.1093/hmg/1.6.397

Turner, G., Webb, T., Wake, S., & Robinson, H. (1996). Prevalence of fragile X syndrome. *American Journal of Medical Genetics, 64*(1), 196–197.

Ullian, E. M., Sapperstein, S. K., Christopherson, K. S., & Barres, B. A. (2001). Control of synapse number by glia. *Science, 291*(5504), 657–61.

Vandenberg, G. G., Dawson, N. J., Head, A., Scott, G. R., & Scott, A. L. (2021). Astrocyte-mediated disruption of ROS homeostasis in Fragile X mouse model. *Neurochemistry International, 146*, 105036. https://doi.org/10.1016/j.neuint.2021.105036

Verkerk, A. J. M. H., Pieretti, M., Sutcliffe, J. S., Fu, Y.-H., Kuhl, D. P. A., Pizzuti, A., Reiner, O., Richards, S., Victoria, M. F., Zhang, F., Eussen, B. E., & Warren, S. T. (1991). Identification

of a gene (FMR-1) containing a CGG repeat coincident with a breakpoint cluster region exhibiting length variation in fragile X syndrome. *Cell, 65*(5), 905–914. https://doi.org/10.1016/0092-8674(91)90397-H

von Kügelgen, I. (2019). Pharmacology of P2Y receptors. *Brain Research Bulletin, 151*, 12–24. https://doi.org/10.1016/j.brainresbull.2019.03.010. Epub 2019 Mar 25 PMID: 30922852.

Wallingford, J., Scott, A. L., Rodrigues, K., & Doering, L. C. (2017). Altered developmental expression of the astrocyte-secreted factors hevin and SPARC in the fragile X mouse model. *Frontiers in Molecular Neuroscience, 10*, 268–268. https://doi.org/10.3389/fnmol.2017.00268

Wink, M. R., Braganhol, E., Tamajusuku, A. S., Casali, E. A., Karl, J., Barreto-Chaves, M. L., Sarkis, J. J., & Battastini, A. M. (2003). Extracellular adenine nucleotides metabolism in astrocyte cultures from different brain regions. *Neurochemistry International, 43*(7), 621–628. https://doi.org/10.1016/S0197-0186(03)00094-9

Youings, S. A., Murray, A., Dennis, N., Ennis, S., Lewis, C., McKechnie, N., Pound, M., Sharrock, A., & Jacobs, P. (2000). FRAXA and FRAXE: The results of a five year survey. *Journal of Medical Genetics, 37*(6), 415–421. https://doi.org/10.1136/jmg.37.6.415

Zhang, R., Watson, D. G., Wang, L., Westrop, G. D., Coombs, G. H., & Zhang, T. (2014). Evaluation of mobile phase characteristics on three zwitterionic columns in hydrophilic interaction liquid chromatography mode for liquid chromatography-high resolution mass spectrometry based untargeted metabolite profiling of Leishmania parasites. *Journal of Chromatography A, 1362*, 168–179. https://doi.org/10.1016/j.chroma.2014.08.039

Zhong, X., Malhotra, R., Woodruff, R., & Guidotti, G. (2001). Mammalian plasma membrane ecto-nucleoside triphosphate diphosphohydrolase 1, CD39, Is not active intracellularly: The N-glycosylation state of CD39 correlates with surface activity and localization*. *Journal of Biological Chemistry, 276*(44), 41518–41525. https://doi.org/10.1074/jbc.M104415200

Zhou, S., Liu, G., Guo, J., Kong, F., Chen, S., & Wang, Z. (2019). Pro-inflammatory effect of downregulated CD73 expression in EAE astrocytes. *Frontiers in Cellular Neuroscience*. https://doi.org/10.3389/fncel.2019.00233

Zimmermann, H. (1996). Biochemistry, localization and functional roles of ecto-nucleotidases in the nervous system. *Progress in Neurobiology, 49*(6), 589–618. https://doi.org/10.1016/0301-0082(96)00026-3